Parametric resonance: a risk to be avoided or an opportunity to be exploited? A case for a 2:1 wave energy converter

Giuseppe Giorgi

Abstract—**A common challenge that unites all players in the wave energy conversion field, both on the academic and industrial sides, is the struggle to increase the converted power output. Along this journey, if devices are discovered prone to parametric resonance, it is usually detrimental for power extraction and potentially threatening the device integrity. In this paper, it is argued that, rather than a risk to be avoided, parametric resonance can be an opportunity to be exploited, to widen the response bandwidth of the system and, ultimately, making more energy available at the power take-off shaft. Since parametric resonance is a highly nonlinear phenomenon induced by time-varying wetted surface, linear models are blind and inept to articulate such an instability. Therefore, nonlinear Froude-Krylov forces are herein implemented, via a computationally convenient approach available for prismatic floaters, that is compatible with real-time computation and exhaustive simulation approaches. A pendulum-based device is considered, purposely designed to exhibit a 2:1 ratio between heave and pitch natural frequencies, which triggers parametric instability. Results show that, as expected, linear models predict a single region of significant potential power extraction close to the pitch natural frequency; conversely, leveraging the designed attitude to develop parametric instability, a second additional region appears close to the heave natural period. Therefore, the free response bandwidth is indeed enlarged, becoming a more fertile baseline for energy-maximising nonlinear control strategies.**

Index Terms—**Wave Energy Converter, 2:1 Parametric Resonance, Nonlinear Froude-Krylov force, Parametric instability, Nonlinear Dynamics.**

I. INTRODUCTION

DESPITE significant technological advances in recent years, the wave energy field still faces the major challenge of reducing the Levelised Cost of Energy (LCoE) to become competitive with other forms of renewable energy and appealing to public and private investors [1], and eventually contribute to the decarbonization of energy systems [2]. On the one hand, effort is directed towards the reduction of capital and operational expenditures: techno-economic optimisations [3] are based on cost functions that, although difficult to be estimated due to a still immature industry [4], are becoming increasingly representative and informative of the real system thanks to bottom-up approaches [5]. On the other hand, the complementary route to LCoE reduction is to increase the overall productivity [6], especially broadening the frequency bandwidth of the device such that it performs well in a wide set of wave conditions [7], and reaches a high capacity factor [8]. The prime tool to increase the energy extraction, especially away from the natural frequency of the system, is optimal control: usually by means of the Power Take-Off (PTO), the control strategy applies an action that intends to modify the free response of the device to achieve the control objective, which normally includes the converted energy.

Figure 1 presents a notional representation of the power extraction of a generic heaving point absorber Wave Energy Converter (WEC), highlighting the baseline of free response with proportional passive control, i.e. a static damping coefficient that simply extracts energy and is not able to significantly modify the dynamics of the WEC. Budal's limits are also represented in order to draw a benchmark of the maximum convertible power due to physical limits [9]. Under ideal conditions where the PTO action can be arbitrary chosen by the control strategy, optimal control can virtually modify the system dynamics to any extent required to optimise performance; Figure 1 shows that optimal control with loose (or no) constraints enables a large leap from the free response up to the proximity of the Budal's limits. However, practical physical constraints (typically on the force, displacement, and/or velocity) limit the scope of effectiveness of the control action, such that the controlled response lies in a neighbourhood of the free response, as narrow as demanding the constraints are; indeed, Fig. 1 shows that a realistic optimal control with tight constraints leads to a much lower improvement with respect to the baseline. Although it is tempting to rely on the optimal control alone to increase the productivity, Fig. 1 suggests that improving the free response baseline is still necessary; therefore, design should also be optimised (ideally in conjunction with control), in order to provide a fertile free response baseline that a realistic (constrained) control can practically lead to optimal power production.

Substantial design modifications, spanning from the working principle and subsystem configurations to the geometry and dimensions, are viable at low Technology Readiness Levels (TRLs), when costs are relatively low and failures are not catastrophic [10]. However, the knowledge of the system may still be superficial at low

Marine Offshore Renewable Energy Lab (MOREnergy Lab), Department of Mechanical and Aerospace engineering (DIMEAS), Politecnico di Torino, Italy, Via Duca degli Abruzzi 24, Turin, 10129, Italy (e-mail: giuseppe.giorgi@polito.it).

Digital Object Identifier:
https://doi.org/10.36688/ewtec-2023-272

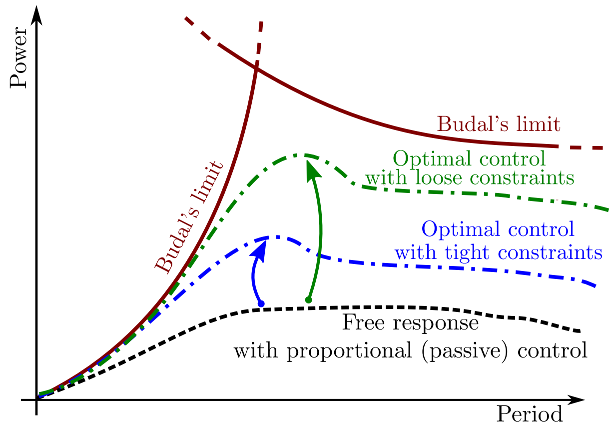

Fig. 1. Notional power extraction for different wave periods of a generic heaving point absorber wave energy converter, including Budal's power extraction limits, free response baseline with passive control, and optimal control with loose and tight constraints.

TRL, since experience is limited and numerical models may not be reliable. Indeed, holistic techno-economic optimisations that modify the design rely on the accuracy of the underlying numerical model, and its effectiveness in a real world application depends on the representativeness of the numerical model [11]. Fidelity is commonly interpreted as a gradient, with gradually higher accuracy for incrementally more complex models [12]; common available models for WECs range from linear potential flow theory [13], with inclusion of correction factors for viscous effects of the wave-structure interaction [14] and potential device-specific nonlinearities [15], to weakly-nonlinear model [16] and fully-nonlinear Computational Fluid Dynamics models [17] used to implement numerical wave tanks [18].

Due to the strict requirement of low computational time, optimisations are implemented with either linear [19], linearized [20], or reduced models [21]; based on the hypothesis that fidelity is a gradient, it is assumed that the real behaviour of the WEC will fall within a given range of error, somewhat proportional to the complexity of the model [13]. However, the accuracy of representation of certain nonlinear phenomena is actually Boolean (yes or no), rather than a gradient, in the sense that they are either articulated or completely overlooked [22]. This is the case of *parametric resonance*.

Parametric resonance is a type of instability, further discussed in Sect. II, that can be appreciated only by models considering time-varying wetted surfaces; therefore, linear models are completely blind to parametric resonance. When present, it is usually discovered (with dismay) well after design, likely in the first experimental tests [23]: it is usually detrimental and mitigation actions are sought [24].

In this paper, it is argued that, if properly embedded early in the design phases, parametric resonance can actually be exploited to improve power conversion capabilities. The reason why this is quite uncommon is that numerical models typically able to articulate parametric resonance are time consuming and not suitable for early design applications. In addition, since parametric resonance may appear under narrow frequency conditions, also fully-nonlinear CFD models may overlook this phenomenon [25]. In this paper, a computationally efficient mathematical formulation is briefly presented and used, based on a recent description of nonlinear Froude-Krylov forces for prismatic floaters [26], which is computationally compatible with early design applications and extensive simulation, as well as an input generator for data-driven system identification approaches.

The remainder of the paper is organized as follows: Section II describes parametric resonance, when it is detrimental (most cases) and a few examples when it is exploited (within and outside wave energy field). Section III proposes a WEC that is purposely designed to be prone to parametric resonance, with the objective to increase the free response bandwidth. Section IV presents the computationally efficient numerical model that can articulate such a nonlinear phenomenon. Finally, Sect. V presents results and discussion, while Sect. VI draws final conclusions.

II. Parametric resonance

Parametric resonance is an internal excitation mechanism activated by time-variations of one or more parameters of the system [27]. Such a phenomenon is usually related to a Mathieu-type of instability [28]. The Mathieu equation is a single degree of freedom (DoF) second-order differential equation of motion of the variable χ, with the stiffness term varying harmonically with time (t) at a given frequency (ω); in real engineering applications, the damped Mathieu equation is considered:

$$\ddot{\chi} + \mu\dot{\chi} + (\Delta + \Lambda \cos\tau)\,\chi = 0, \tag{1}$$

where the time-derivatives are with respect to the dimensionless $\tau = \omega t$, Δ represents a dimensionless stiffness, Λ is the dimensionless amplitude of the stiffness variation, and μ is the dimensionless damping coefficient. The stability diagram of equation (1) is shown in Fig. 2, where $\Delta^2 = \omega_n/\omega$ and ω_n is the natural frequency of the 1-DoF system; two conditions for instability (shaded areas in Fig. 2) arise:

1) The excitation frequency (ω) is twice of or equal to the natural frequency (ω_n) of the system ($\Delta = 0.25$ or 1, respectively)
2) The excitation amplitude exceeds internal dissipations of the system (increasing Λ)

The Mathieu equation can give precious insight to grasp an overall understanding of the conditions triggering parametric resonance, which in turn can lead design choices (as discussed in Sect. II); however, it is not applicable to predict the severity of the parametric response, especially because there is no straightforward correspondence between the coefficients of equation (1) and the physical phenomenon. In fact, the variations of the stiffness term are, in general, not harmonic, but depend on the intersection of the floater and the wave field. Moreover, similar nonlinearities are present in the wave excitation force. Finally, 6-DoF systems are likely

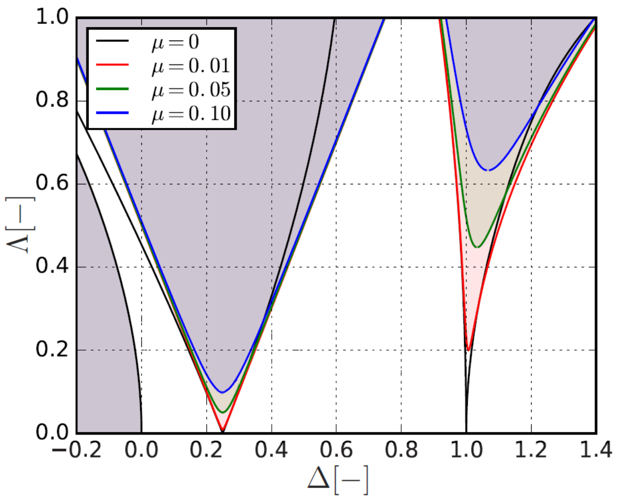

Fig. 2. Stability diagram of the damped Mathieu equations (μ is the damping), shown in (1). Unstable regions are shaded; they arise when the excitation frequency is twice ($\Delta = 0.25$) of or equal ($\Delta = 1$) to the natural frequency of the system, and for sufficiently large excitation amplitude (increasing Λ). Adapted from [29].

to entail complex energy exchanges between different modes of motion. Therefore, a dedicated numerical model is developed in Sect. IV.

The following subsections briefly mention how parametric resonance is perceived: the vast majority of applications consider it as detrimental, hence a *risk* to be avoided, as discussed in Sect. II-A; conversely, Sect. II-B presents some examples, apart from the present paper, where parametric resonance is leveraged as an enabling phenomena to improve performance, hence treated as an *opportunity*.

A. A risk to be avoided?

Parametric resonance is a widely known phenomenon in classic ocean engineering [28], carefully evaluated because of the great economic and safety issues it entails. It is of particular interest for large cargo ships, since unsuppressed parametric roll instability can lead to loss of transported goods and potential harm to the crew; therefore, various methods for detection and prevention of parametric rolling are developed and implemented [30]. Similarly, spar-like structures are prone to experience parametric resonance [31], with consequent large rotations. Therefore, parametric resonance is not desirable, since such structures are expected to experience small rotations to be fit for purpose (typically oil or floating offshore wind); in addition, the station keeping system should be designed with proper knowledge of the types of motions during operation.

In the wave energy field, parametric resonance has been observed in a few floating systems, composed by either one tethered body or a self-referenced two-body system: in a floating sloped WEC [32], in a pendulum-based self-referenced device [33], in a floating oscillating water column [34], in a bottom-tethered device [35], and in a two-body self-referenced device [36]. In all of such instances, parametric resonance decreases the energy conversion efficiency, since it internally diverts part of the energy *away* from the degree of freedom (DoF) where the PTO is installed, hence reducing the available energy. In addition, higher and potentially unexpected loads may be transferred to other subsystems of the WEC, particularly on the mooring system, increasing chances of damage and reducing reliability. Therefore, dedicated detection and suppression strategies are put in place to avoid the rise or parametric instability [37].

B. An opportunity to be exploited?

If properly embedded in early design phases, parametric resonance can be an opportunity to broaden the bandwidth and increase power extraction for the following two main reasons:

i) Parametric resonance can be used to internally reroute part of the energy *towards* the DoF where the PTO is installed, increasing the amount of available energy.
ii) Instabilities grow exponentially, compatibly with the damping of the system.

Outside of the wave energy field, in particular in the mechanical vibration energy harvesting (VEH) field, it is common that nonlinearities and instabilities are the founding working principles of the system, rather than a burden. In fact, linear VEHs typically have a sharp and narrow frequency response curve, which would not make energy generation economically viable. With the objective to broaden their bandwidth, popular expedients are to introduce nonlinearities in the system [38]: Duffing nonlinearity [39], bistability [40], parametric oscillators [41], stochastic oscillators [42], among others. One of the reasons why instability-based working principles are so popular in the VEH field is mainly the simplicity of the underlying nonlinear mathematical model, which normally is algebraic and fully-white (i.e., transparently based on physical quantities).

There exist a few examples of WECs that exploit parametric resonance to extract energy. The majority of concepts are based on the inertial coupling between a floater and one [43] or more [44] pendula; in some concepts, rotation control may be required to initiate and maintain the parametric rotation [45], potentially implemented via length adjustments [46]. A single floater system is considered in [47], where a control strategy is able to take into account the nonlinear hydrodynamic coupling between heave and surge/pitch, such that the energy extracted from heave is increased. Finally [48] considers a WEC with two concentric floaters, where parametric resonance is induced by the modulation of the mass.

III. A 2:1 Parametric Resonance Pitching WEC

This paper focuses on WECs that extract energy from the pitching motion of a floater, either directly (e.g., via a fixed reference super-structure) or indirectly (e.g., via inertial coupling with an inner mechanisms); numerical results are produced for a case study with inertial coupling, although notional considerations are more general.

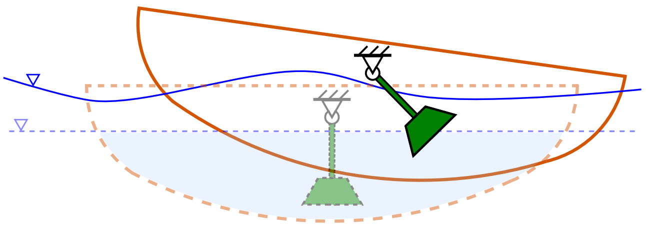

Fig. 3. Schematics of the PeWEC-like wave energy converter, with a pendulum contained within a sealed hull. The dashed transparent body is at rest position in still water, while the solid lines represent a displaced position in sea water.

Evidences from [47] or [49] have shown that, although linearly independent, heave and pitch DoFs are hydrodynamically coupled once the instantaneous wetted surface is taken into account in the computation of the excitation forces, particularly in the nonlinear Froude-Krylov component. Therefore, the present paper argues that a WEC specifically designed to have a 2:1 ratio between heave and pitch natural frequency would greatly benefit from the consequently induced parametric resonance. In fact, under parametric instability conditions (Sect. III), a portion of the incoming energy would be channelled from the heave DoF to the the pitch DoF, hence made available to be converted by the PTO.

In order to test such an assumption, as well to provide preliminary quantitative results about the significance of the benefits, if any, a case study is herein formulated. The Pendulum Wave Energy Converter (PeWEC) is considered as a baseline [50], which is a sealed floater containing a pendulum: as the hull pitches in response to incoming waves, the oscillations of the pendulum due to the inertial coupling are dampened by the PTO. A schematics of a PeWEC-like device is presented in Fig. 3. The geometry, dimensions, and mass properties of the PeWEC-like device are inspired by [49] and [51]; however, the pitching inertia of the system is artificially modified such that the heave natural period (T_3) would be half the pitch natural period (T_5), i.e. a 2:1 ratio between the respective natural frequencies.

IV. Mathematical modelling

The purpose of this paper is to specifically study the effect of parametric resonance due to the nonlinear coupling between heave and pitch degrees of freedom. Therefore, the mathematical model and setup is carefully chosen to enable meaningful and unambiguous considerations; in particular, confounding factors are eliminated to guarantee a clear, transparent and univocal inference of causality. Therefore, the following simulation conditions are identified:

- *Monochromatic waves*: Since parametric resonance is a frequency-dependent phenomenon, regular waves are considered to clearly discriminate trends in the dynamic response of the system.
- *Time-domain model*: described in Sect. IV-A, it is necessary to numerically solve nonlinear systems in the time domain.
- *Nonlinear Froude-Krylov (NLFK) force*: it is the only nonlinearity included in the system, described in Sect. IV-B, since it can articulate parametric resonance; all other nonlinear effects are neglected (i.e., viscosity, PTO saturations, pendulum kinematics, moorings, etc.), so that any nonlinear behaviour is univocally due to NLFK.
- *Only heave and pitch hydrodynamic DoFs*: being linearly uncoupled, any coupling in the nonlinear response depends only on parametric resonance, which activates an internal energy exchange between such DoFs; note that simulating surge would have been a confounding factor, since it would have introduced a linear coupling with pitch, hence an additional direction of energy flow, as well as required an additional station-keeping term in the equation of motion.
- *No PTO*: as discussed in Sect. I, considering the free response of the device is crucial to articulate its inherent characteristics, which can then be leveraged by an appropriate control system.

A. Time domain model

Two time-domain models are herein considered, with the only difference being the inclusion of linear (LFK) or nonlinear (NLFK) static and dynamic Froude Krylov forces. Regular waves are considered, whose periods and heights are chosen considering a typical bivariate distribution [52]. The linear equation of motion, defined about the center of gravity, is written in the frequency domain as follows:

$$\left[-\omega^2\left(\mathbf{M}+\mathbf{A}(\omega)\right)+j\omega\mathbf{B}(\omega)+\mathbf{K}_h\right]\boldsymbol{\xi}_2=\mathbf{F}_d+\mathbf{F}_{FK_d} \tag{2}$$

where $\boldsymbol{\xi}_2$ is the 2×1 state vector, composed of heave (z) and pitch (θ), $\mathbf{M}$ the diagonal inertia matrix, $\mathbf{A}(\omega)$ and $\mathbf{B}(\omega)$ the diagonal frequency-dependent added mass and radiation damping, $\mathbf{K}_h$ the diagonal linear hydrostatic stiffness, $\mathbf{F}_d$ and $\mathbf{F}_{FK_d}$ are the diffraction and linear dynamic FK forces. The linear hydrodynamic curves are computed for the mean wetted surface of the floater via a linear Boundary Element Method (BEM) software, such as Nemoh [53] or WAMIT [54]. The NLFK version of (2) alternatively computes $(\mathbf{F}_{FK_d} - \mathbf{K}_h\boldsymbol{\xi}_2)$ in a nonlinear way, as described in Sect. IV-B.

The frequency domain equation is converted into time domain, substituting the radiation frequency domain components by their time-domain state-space approximation, identified via the FOAMM toolbox [55], [56]. In addition, the 2-DoF equation for the hydrodynamic interaction of the waves with the hull is augmented to include the force exchange between the hull and the swinging pendulum; therefore, the 2-DoF state vector $\boldsymbol{\xi}_2$ is augmented to $\boldsymbol{\xi}_3$ by appending the rotation (ε) of the pendulum about its hinge. The hull-pendulum interactions are linearized as in [51], resulting in additional terms in the total inertial and stiffness matrices of the augmented system.

B. Nonlinear Froude-Krylov force model

Since parametric resonance is due to time-varying parameters of the system, nonlinear Froude-Krylov forces are best suited numerical tools; in fact, NLFK forces are computed as the integral of the pressure of the undisturbed wave field onto the instantaneous wetted surface. As mentioned in Sect. I, applications based on real-time simulated results and/or several iterations in a short time, require models with an adequately low computational cost. While geometries of arbitrary complexity may require mesh-based NLFK methods, often computationally demanding, axisymmetric and prismatic floaters can benefit from a computationally effective analytical description of the NLFK integrals. The PeWEC-like device is indeed prismatic, i.e. its geometry is invariant in the horizontal direction perpendicular to the wave propagation and parallel to the wave front.

Although throughout details of the NLFK integration method for prismatic floaters are given in [49], a brief summary is presented hereafter. Assuming two-dimensional waves in the (x, z) coordinate system, where x is the direction of propagation of the wave, and z is the vertical axis, positive upwards, with the origin at the (SWL), a the wave amplitude, ω the wave frequency, k the wave number, h the water depth, and z' the vertical coordinate modified according to Wheeler's stretching [57], the total undisturbed pressure (p_u) follows:

$$p_u = -\rho g z + a\cos(\omega t - kx)\,\frac{\cosh(k(z'+h))}{\cosh(kh)}, \qquad (3)$$

where ρ is the water density, g the acceleration of gravity.

Froude-Krylov generalized forces $(\mathbf{F}_{FK})$, divided into linear forces $(\mathbf{f}_{FK})$ and torques $(\boldsymbol{\tau}_{FK})$, integrate the undisturbed pressure field (p_u), shown in (3), as follows:

$$\mathbf{f}_{FK}(t) = \mathbf{f}_g + \iint_{S_w(t)} p_u(x,y,z,t)\ \mathbf{n}\ dS, \qquad (4a)$$

$$\boldsymbol{\tau}_{FK}(t) = (\mathbf{r}_g - \mathbf{r}_R)\times\mathbf{f}_g + \iint_{S_w(t)} p_u(x,y,z,t)\ (\mathbf{r}-\mathbf{r}_R)\times\mathbf{n}\ dS, \qquad (4b)$$

where $\mathbf{f}_g$ is the gravity force, $\boldsymbol{\tau}_g$ its contribution to the torque, $\mathbf{n}$ is the unity vector normal to the surface, $\mathbf{r}$ is the generic position vector, $\mathbf{r}_R = (x_R, y_R, z_R)'$ is the reference point around which the torque is computed, and likewise $\mathbf{r}_g$ is the position vector of the centre of gravity.

While generic NLFK solvers for arbitrary complex floaters must rely on a meshed representation of $S_w(t)$, which becomes the computational bottleneck, a faster analytical representation, already available for axisymmetric floaters [58], [59], can be readily obtained also for prismatic floaters. Figure 4 shows a snapshot obtained with such an analytical representation, highlighting how significantly the instantaneous wetted surface changes with respect to the rest position.

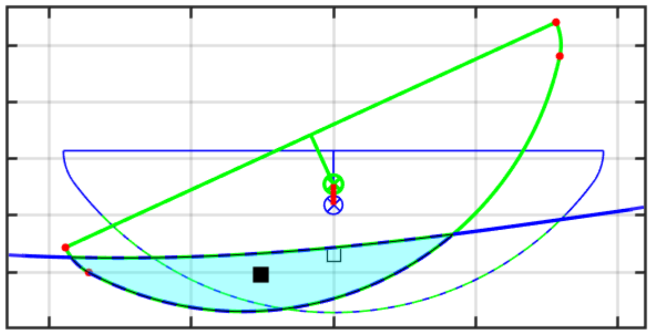

Fig. 4. Snapshot of a displaced hull, shown in green thick solid line, with instantaneous free surface elevation, shown in blue thick solid line, enclosing the instantaneous submerged volume (shaded area). The crossed-circle marker shows the position of the centre of gravity, while the square shows the centre of buoyancy (empty: LFK; full: NLFK). The rest position (LFK) is shown in thin line. Adapted from [26].

Within a body-fixed frame, a generic point $\hat{\mathbf{r}}$ belonging to the external surface of a prismatic body invariant in the $\hat{y}$ direction can be mapped by a change of coordinates $\mathbb{R}^3 \mapsto \mathbb{R}^2$ as:

$$\hat{\mathbf{r}}: \begin{cases} \hat{x} = \gamma_x(\alpha) \\ \hat{y} = \hat{y} \\ \hat{z} = \gamma_z(\alpha) \end{cases}, \quad \alpha \in [\alpha_1, \alpha_2] \wedge \hat{y} \in [\hat{y}_1, \hat{y}_2] \qquad (5)$$

where γ_x and γ_z are generic parametric curves, and α is the sweep parameter. Typically, but not necessarily, α goes from 0 to 1 as the directional curve moves from one to the other end. The parametric formulation enables the use of arbitrary complex cross-sections of the prismatic body.

Finally, thanks to the analytical description in (5) and appropriate mapping between world frame and body-fixed frame, it is possible to entirely define all terms in the integral formulation in (4), which is then solved numerically.

V. Results and discussion

Time-domain simulations are performed for a dense grid of monochromatic waves, sweeping wave periods (T_w) and wave heights (H_w) to include relevant operational conditions. In particular, in order to highlight parametric resonance behaviour, T_w ranges from 0.25 to 1.4 times the natural period in pitch (T_5); similarly, H_w is defined as a ratio of the draft (D) of the floater at rest, ranging from 0 to 1. Time-domain simulations are performed for long enough that the response is ensured to be steady and periodic; in order to smooth the initial transient, a sigmoid weight from 0 to 1 is applied during the first 5 wave periods of the incoming free surface elevation. The resulting amplitude of motion is computed as the difference between peak and trough of the signal over a time window taken at the end of the simulation; the length of the time window is $2T_w$, to appreciate the expected frequency doubling, due to parametric resonance. Figure 5 presents such amplitudes in normalized heave (z/D), pitch (θ), and the pendulum oscillation (ε), plotted with respect to the

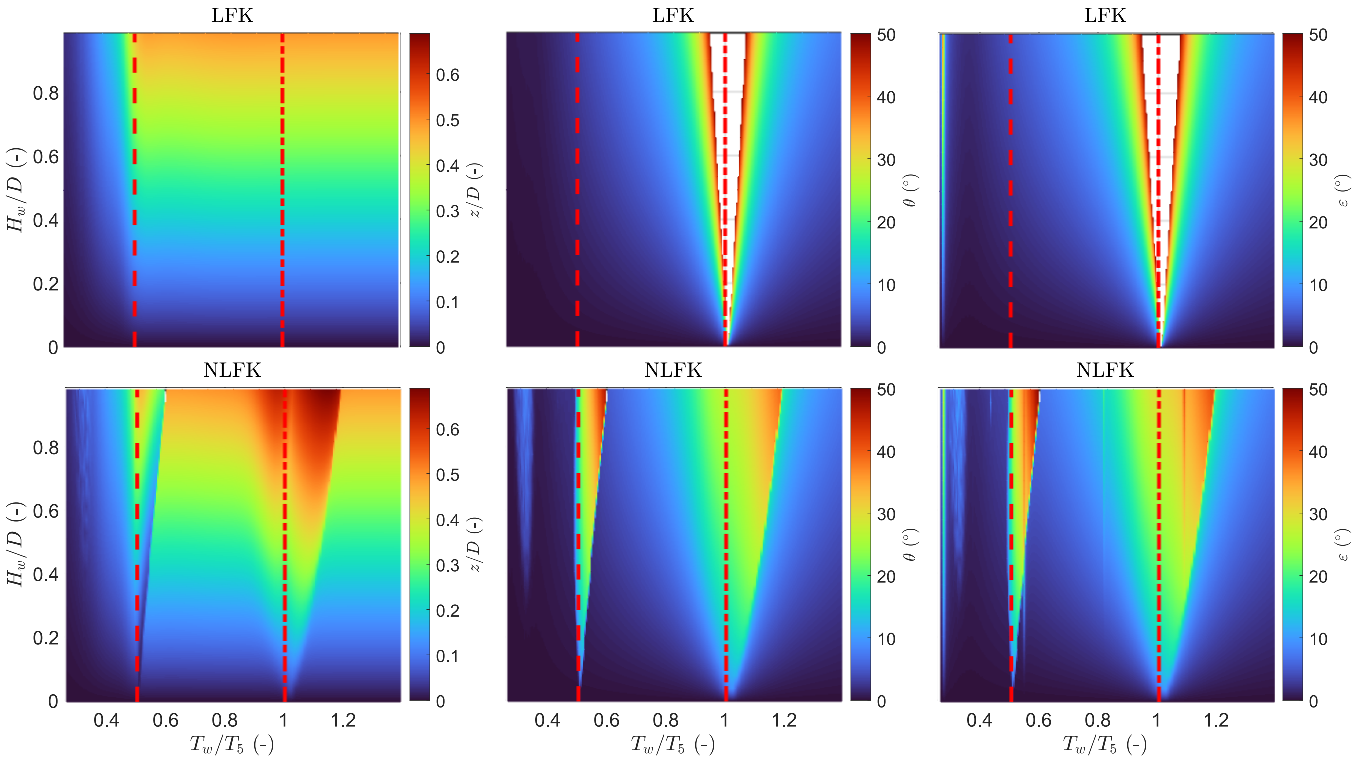

Fig. 5. From left to right: amplitudes in normalized heave (z/D), pitch (θ), and the pendulum oscillation (ε), plotted with respect to the normalized wave period (T_w/T_5) and normalized wave height (H_w/D); top and bottom rows refer to LFK and NLFK models, respectively. The dashed and dash-dotted lines highlight T_w/T_5 equal to 0.5 and 1, respectively.

normalized wave period (T_w/T_5) and normalized wave height (H_w/D), according to LFK and NLFK models. Meaningful ratios of T_w/T_5 are highlighted with 2 red lines: a dash-dotted line is located at $T_w = T_5$, whereas a dashed line highlights $T_w = T_3 = 0.5T_5$, following the 2:1 resonance condition imposed in Sect. III, i.e. both the heave natural period and the simplified parametric resonance condition.

The linear response (top row of Fig. 5) presents no coupling between heave and pitch, as expected. Both heave and pitch responses reach their peak at their respective natural frequencies ($T_w = T_3 = 0.5T_5$ and $T_w = T_5$, respectively); the pendulum oscillation follows directly the pitching response, thanks to the inertial coupling. According to the hypothesis discussed in Sect. IV, the LFK model is fully linear and not dampened, and no saturation or end-stop is included in the simulation; it follows that unrealistic responses are obtained close to the pitching natural frequency. Therefore, to improve readability and enable meaningful discussion, any oscillation above 50° is not plotted in Fig. 5 (white area).

The nonlinear response (bottom row of Fig. 5) is presented with the same color bar scale of the LFK model, to facilitate qualitative comparison of the resulting amplitudes of motion. It is evident that a nonlinear coupling appears at both highlighted normalized wave periods. In particular, at $T_w = 0.5T_5$, the heave response decreases with respect to the LFK model, with a clear wedge incision in the response scatter; the same wedge is found in the θ and ε responses, highlighting how parametric resonance effectively redirects part of the energy away from the heaving DoF. It is worth noting that, at this frequency, the linear model predicts close to no response, remarking that parametric resonance is the one and only excitation mechanism, introduced thanks to the 2:1 ratio prescribed in the design stage (see Sect. III).

As H_w increases, the wedge appears asymmetric with respect to the vertical line $T_w = 0.5T_5$: while the left edge remains vertical, the right edge shifts at higher periods; it follows that the parametric resonance response range increases and, being more energy available at higher H_w, the amplitude of the response increases accordingly. This behaviour is consistent with the qualitative prediction of the Mathieu diagram, shown in Fig. 1, where the width of the instability region increases for higher incoming energy, once the internal damping of the system is overcome.

Similarly, nonlinear coupling also appears at $T_w = T_5$; however, inverse energy flow is obtained in this case, since the heave response is higher at $T_w = T_5$ than in its neighbourhood. Based on the simulation conditions, it is not possible to assess if this is detrimental or beneficial to energy extraction, since the LFK response in pitch is unrealistic and cannot provide a meaningful benchmark. If the total mechanical energy absorbed by the whole system is assumed to be constant, parametric resonance drains some energy from pitch to obtain a higher heaving response, so it would be detrimental. However, parametric instability may induce an overall higher response, hence making more mechanical energy available at the floater; in this case, parametric resonance may still have a net positive effect at the PTO axis, despite the higher heave response.

It is also worth noting that the pitch, and conse-

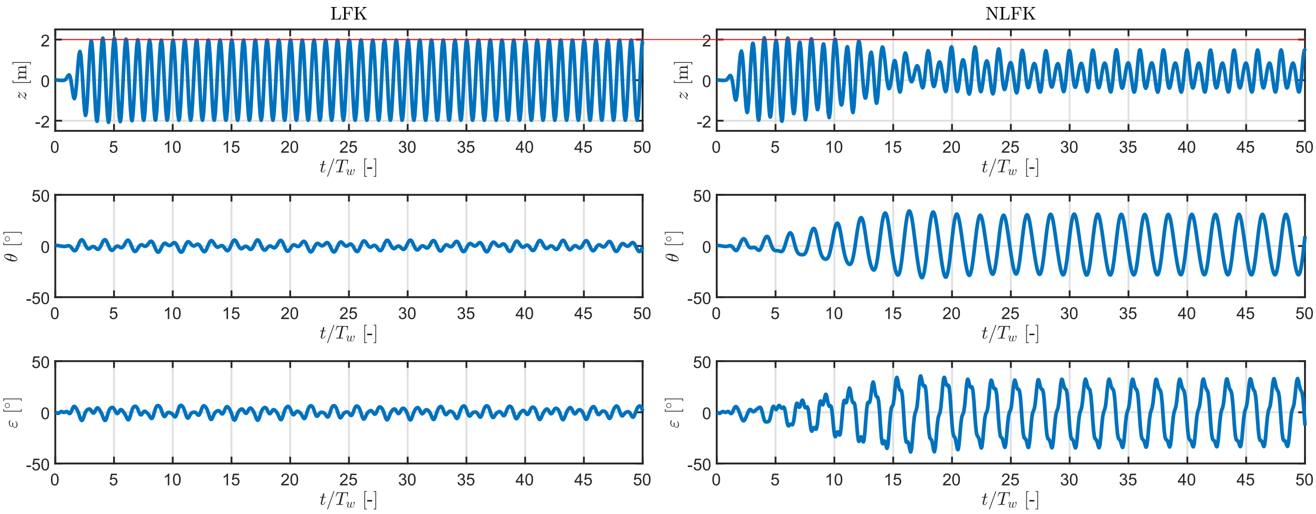

Fig. 6. Time trace of the dynamic response at $T_w = 0.55T_5$ and $H_w = 4$m, according to the LFK (left) and NLFK (right) models. A sigmoid ramp is applied to the incoming free surface elevation.

quently the pendulum oscillation, are lower than the LFK prediction, and never take unrealistic values. This is a direct consequence of using a representative NLFK model, which takes into account the actual instantaneous wetted surface of the floater.

Finally, Fig. 5 shows that inducing parametric resonance has had the effect of enlarging the potential bandwidth of available energy conversion, since the PTO axis is excited in a wider range of wave periods, i.e. close to $0.5T_5$ and T_5. Such a modification of the free response of the system can be leveraged by a control strategy if an only if its underlying numerical model is able to articulate parametric resonance (if model-based controllers are used). Such a nonlinear controller could act on the system to trigger parametric instability, and eventually enhance the severity of parametric response. However, embedding complex nonlinearities into a control-oriented numerical model is a challenging task: promising approaches are based on identification data-driven techniques, already proven to be effective with NLFK-type of nonlinearities [60].

While Fig. 5 presents a comprehensive overview of the WEC response over a wide range of wave conditions, it is worth analysing a representative example of time trace. Figure 6 shows the response in parametric resonance conditions, particularly at $T_w = 0.55T_5$ and $H_w = 4$m. On the left hand-side (LFK), the linear response is mainly in heave, at a single frequency, equal to the excitation wave frequency; pitch and pendulum responses are coupled and negligible. Conversely, the nonlinear response, on the right hand-side (NLFK), clearly shows the process of coupling between heave and pitch. In particular, during the first 10 wave periods, pitch is negligible and the nonlinear and linear heave responses are similar, as highlighted by the horizontal red line; however, parametric resonance gradually drains energy away from heave and towards pitch such that, after the transient is elapsed ($t > 20T_w$), heave is significantly lower while pitch is high. Moreover, note that the steady-state heave response exhibits a clear nonlinear frequency doubling.

In order to better visualize the change in available energy, and the transfer from heave to pitch DoFs, Fig. 7 plots the instantaneous kinetic energy in heave ($E_{k,z}$) and pitch ($E_{k,\theta}$), for the same wave as in Fig. 6. During the first transient, while pitch is negligible, LFK and NLFK heave kinetic energies are similar; however, the kinetic energy in pitch gradually increases as parametric instability builds up, significantly reducing the kinetic energy in heave.

VI. Conclusion

This papers elaborates on the role of parametric resonance in wave energy converters: usually seen as detrimental and undesirable, if properly embedded into the underlying working principle and in early design phases, parametric resonance can potentially become an enabling factor to increase the conversion bandwidth and efficiency. Based on this rationale, a 2:1 parametric resonance WEC is herein proposed, where the natural period in one degree of freedom is purposely tuned to be twice that of another degree of freedom, such that a nonlinear hydrodynamic coupling is used to redirect part of the external energy towards the power take-off system.

Exploiting this potential requires to appropriately address challenges in the mathematical modelling and energy-maximisation control. Computationally efficient mathematical models are required to steer the design at early stages; parametric resonance can be articulated only by models considering time-varying wetted surface. Therefore, this paper implements a computationally convenient formulation of nonlinear Froude-Krylov forces, available for axisymmetric and prismatic floaters.

Thanks to the 2:1 design and to the appropriate numerical model, this papers quantitatively confirms that indeed parametric resonance does appear at the predicted conditions, and it is also meaningful: in fact, the free response of the system shows a significant

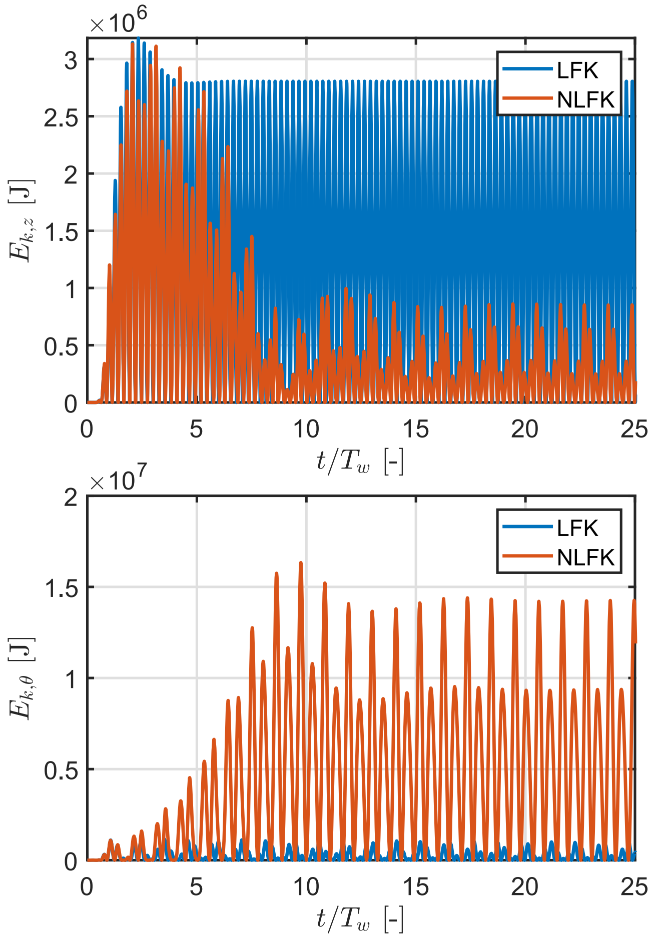

Fig. 7. Instantaneous kinetic energy in heave (top) and pitch (bottom) for a wave with $T_w = 0.55T_5$ and $H_w = 4$m.

increase in the available mechanical energy at the power take-off.

In conclusion, this paper provides evidences that the free response has been indeed improved. However, parametric resonance has only provided a more fertile baseline with higher available energy; it is the role of an appropriate nonlinear control to actually exploit this potential for a final higher power output.

References

[1] A. Vargiu, R. Novo, C. Moscoloni, E. Giglio, G. Giorgi, and G. Mattiazzo, "An Energy Cost Assessment of Future Energy Scenarios: A Case Study on San Pietro Island," *Energies*, vol. 15, no. 13, p. 4535, 2022.

[2] R. Novo, P. Marocco, G. Giorgi, A. Lanzini, M. Santarelli, and G. Mattiazzo, "Planning the decarbonisation of energy systems: The importance of applying time series clustering to long-term models," *Energy Conversion and Management: X*, vol. 15, no. January, p. 100274, 2022.

[3] M. Rava, P. Dafnakis, V. Martini, G. Giorgi, V. Orlando, G. Mattiazzo, G. Bracco, and A. Gulisano, "Low-Cost Heaving Single-Buoy Wave-Energy Point Absorber Optimization for Sardinia West Coast," *Journal of Marine Science and Engineering*, vol. 10, no. 3, 2022.

[4] P. Ruiz-Minguela, D. R. Noble, V. Nava, S. Pennock, J. M. Blanco, and H. Jeffrey, "Estimating Future Costs of Emerging Wave Energy Technologies," *Sustainability 2023, Vol. 15, Page 215*, vol. 15, no. 1, p. 215, dec 2022.

[5] E. Giglio, E. Petracca, B. Paduano, C. Moscoloni, G. Giorgi, and S. A. Sirigu, "Estimating the Cost of Wave Energy Converters at an Early Design Stage: A Bottom-Up Approach," *Sustainability 2023, Vol. 15, Page 6756*, vol. 15, no. 8, p. 6756, apr 2023.

[6] D. Son and R. W. Yeung, "Optimizing ocean-wave energy extraction of a dual coaxial-cylinder WEC using nonlinear model predictive control," *Applied Energy*, vol. 187, pp. 746–757, feb 2017.

[7] Q. Li, X. Li, J. Mi, B. Jiang, S. Chen, and L. Zuo, "A tunable wave energy converter using variable inertia flywheel," *IEEE Transactions on Sustainable Energy*, 2020.

[8] O. Choupin, A. Têtu, B. Del Río-Gamero, F. Ferri, and J. Kofoed, "Premises for an annual energy production and capacity factor improvement towards a few optimised wave energy converters configurations and resources pairs," *Applied Energy*, vol. 312, p. 118716, apr 2022.

[9] J. Falnes and J. Hals, "Heaving buoys, point absorbers and arrays," *Philosophical Transactions of the Royal Society A: Mathematical, Physical and Engineering Sciences*, vol. 370, no. 1959, pp. 246–277, jan 2012.

[10] D. Bull, R. Costello, A. Babarit, K. Nielsen, B. Kennedy, C. Bittencourt Ferreira, J. Roberts, and J. Weber, "Scoring the Technology Performance Level (TPL) Assessment," *Proceedings of the Twelfth European Wave and Tidal Energy Conference*, pp. 1115–1–9, 2017.

[11] E. Faraggiana, G. Giorgi, M. Sirigu, A. Ghigo, G. Bracco, and G. Mattiazzo, "A review of numerical modelling and optimisation of the floating support structure for offshore wind turbines," *Journal of Ocean Engineering and Marine Energy*, vol. 8, no. 3, pp. 433–456, 2022.

[12] J. Davidson and R. Costello, "Efficient Nonlinear Hydrodynamic Models for Wave Energy Converter Design — A Scoping Study," pp. 1–65, 2020.

[13] E. J. Ransley, S. A. Brown, M. Hann, D. M. Greaves, C. Windt, J. Ringwood, J. Davidson, P. Schmitt, S. Yan, J. X. Wang, J. H. Wang, Q. Ma, Z. Xie, G. Giorgi, J. Hughes, A. Williams, I. Masters, Z. Lin, H. Chen, L. Qian, Z. Ma, Q. Chen, H. Ding, J. Zang, J. van Rij, Y.-H. Yu, Z. Li, B. Bouscasse, G. Ducrozet, and H. Bingham, "Focused wave interactions with floating structures: a blind comparative study," *Proceedings of the Institution of Civil Engineers - Engineering and Computational Mechanics*, vol. 174, no. 1, pp. 46–61, mar 2021.

[14] L. S. P. Da Silva, B. S. Cazzolato, ·. Nataliia, Y. Sergiienko, B. Ding, H. M. Morishita, ·. Celso, and P. Pesce, "Statistical linearization of the Morison's equation applied to wave energy converters," vol. 6, pp. 157–169, 2020.

[15] S. A. Sirigu, F. Gallizio, G. Giorgi, M. Bonfanti, G. Bracco, and G. Mattiazzo, "Numerical and Experimental Identification of the Aerodynamic Power Losses of the ISWEC," *Journal of Marine Science and Engineering 2020, Vol. 8, Page 49*, vol. 8, no. 1, p. 49, jan 2020.

[16] L. Letournel, C. Chauvigné, B. Gelly, A. Babarit, G. Ducrozet, and P. Ferrant, "Weakly nonlinear modeling of submerged wave energy converters," *Applied Ocean Research*, vol. 75, no. March, pp. 201–222, 2018.

[17] P. Casalone, O. Dell'Edera, B. Fenu, G. Giorgi, S. A. Sirigu, and G. Mattiazzo, "Unsteady RANS CFD Simulations of Sailboat's Hull and Comparison with Full-Scale Test," *Journal of Marine Science and Engineering 2020, Vol. 8, Page 394*, vol. 8, no. 6, p. 394, may 2020.

[18] C. Windt, J. Davidson, and J. V. Ringwood, "High-fidelity numerical modelling of ocean wave energy systems: A review of computational fluid dynamics-based numerical wave tanks," *Renewable and Sustainable Energy Reviews*, vol. 93, pp. 610–630, oct 2018.

[19] A. Garcia-Teruel, B. DuPont, and D. I. Forehand, "Hull geometry optimisation of wave energy converters: On the choice of the optimisation algorithm and the geometry definition," *Applied Energy*, vol. 280, p. 115952, dec 2020.

[20] M. Bonfanti and G. Giorgi, "Improving Computational Efficiency in WEC Design: Spectral-Domain Modelling in Techno-Economic Optimization," *Journal of Marine Science and Engineering 2022, Vol. 10, Page 1468*, vol. 10, no. 10, p. 1468, oct 2022.

[21] N. Faedo, F. J. Dores Piuma, G. Giorgi, and J. V. Ringwood, "Nonlinear model reduction for wave energy systems: a moment-matching-based approach," *Nonlinear Dynamics*, vol. 102, no. 3, pp. 1215–1237, nov 2020.

[22] G. Giorgi, J. Davidson, G. Habib, G. Bracco, G. Mattiazzo, and T. Kalmár-Nagy, "Nonlinear Dynamic and Kinematic Model of a Spar-Buoy: Parametric Resonance and Yaw Numerical Instability," *Journal of Marine Science and Engineering 2020, Vol. 8, Page 504*, vol. 8, no. 7, p. 504, jul 2020.

[23] K. R. Tarrant and C. Meskell, "Investigation on parametrically excited motions of point absorbers in regular waves," *Ocean Engineering*, vol. 111, pp. 67–81, 2016.

[24] J. Davidson, T. Kalmar-Nagy, and G. Habib, "Parametric excitation suppression in a floating cylinder via dynamic vibration absorbers : a comparative analysis," *Nonlinear Dynamics*, vol. 110, no. 2, pp. 1081–1108, 2022.

[25] J. Palm, L. Bergdahl, and C. Eskilsson, "Parametric excitation of moored wave energy converters using viscous and non-viscous CFD simulations," in *Renew*, no. October, 2018.

[26] G. Giorgi, S. Sirigu, M. Bonfanti, G. Bracco, and G. Mattiazzo, "Fast nonlinear Froude–Krylov force calculation for prismatic floating platforms: a wave energy conversion application case," *Journal of Ocean Engineering and Marine Energy*, vol. 7, no. 4, pp. 439–457, nov 2021.

[27] G. Habib, G. Giorgi, and J. Davidson, "Coexisting attractors in floating body dynamics undergoing parametric resonance," *Acta Mechanica*, vol. 233, no. 6, pp. 2351–2367, jun 2022.

[28] T. I. Fossen and H. Nijmeijer, *Parametric resonance in dynamical systems*. Springer, 2012.

[29] G. Giorgi, R. P. F. Gomes, G. Bracco, and G. Mattiazzo, "Numerical investigation of parametric resonance due to hydrodynamic coupling in a realistic wave energy converter," *Nonlinear Dynamics*, 2020.

[30] N. Umeda, H. Hashimoto, ·. S. Minegaki, A. Matsuda, N. Umeda, H. Hashimoto, S. Minegaki, and A. Matsuda, "An investigation of different methods for the prevention of parametric rolling," *J Mar Sci Technol*, vol. 13, pp. 16–23, 2008.

[31] H. K. Jang and M. H. Kim, "Mathieu instability of Arctic Spar by nonlinear time-domain simulations," *Ocean Engineering*, vol. 176, pp. 31–45, mar 2019.

[32] G. S. Payne, J. R. Taylor, T. Bruce, and P. Parkin, "Assessment of boundary-element method for modelling a free-floating sloped wave energy device. Part 2: Experimental validation," *Ocean Engineering*, vol. 35, no. 3-4, pp. 342–357, mar 2008.

[33] J. Cordonnier, F. Gorintin, A. De Cagny, A. H. Clément, and A. Babarit, "SEAREV: Case study of the development of a wave energy converter," *Renewable Energy*, vol. 80, pp. 40–52, aug 2015.

[34] R. Gomes, J. Henriques, L. Gato, and A. Falcão, "Time-domain simulation of a slack-moored floating oscillating water column and validation with physical model tests," *Renewable Energy*, vol. 149, pp. 165–180, apr 2020.

[35] J. Orszaghova, H. Wolgamot, S. Draper, R. Eatock Taylor, P. H. Taylor, and A. Rafiee, "Transverse motion instability of a submerged moored buoy," *Proceedings of the Royal Society A: Mathematical, Physical and Engineering Sciences*, vol. 475, no. 2221, 2019.

[36] A. Kurniawan, M. Grassow, and F. Ferri, "Numerical modelling and wave tank testing of a self-reacting two-body wave energy device," *Ships and Offshore Structures*, vol. 14, no. sup1, pp. 344–356, oct 2019.

[37] J. Davidson and T. Kalmár-nagy, "A Real-Time Detection System for the Onset of Parametric Resonance in Wave Energy Converters," *Journal of Marine Science and Engineering*, vol. 8, no. 819, pp. 1—-23, 2020.

[38] Y. Jia, "Review of nonlinear vibration energy harvesting: Duffing, bistability, parametric, stochastic and others," *Journal of Intelligent Material Systems and Structures*, vol. 31, no. 7, pp. 921–944, 2020.

[39] A. Bahrami and M. Tayarani, "Chaotic Behavior of Duffing Energy Harvester," *Energy Harvesting and Systems*, vol. 5, no. 3-4, pp. 67–71, sep 2018.

[40] D. Liu, Y. Wu, Y. Xu, and J. Li, "Stochastic response of bistable vibration energy harvesting system subject to filtered Gaussian white noise," *Mechanical Systems and Signal Processing*, vol. 130, pp. 201–212, sep 2019.

[41] G. Giorgi and N. Faedo, "Performance enhancement of a vibration energy harvester via harmonic time-varying damping: A pseudospectral-based approach," *Mechanical Systems and Signal Processing*, vol. 165, p. 108331, feb 2022.

[42] C. R. McInnes, D. G. Gorman, and M. P. Cartmell, "Enhanced vibrational energy harvesting using nonlinear stochastic resonance," *Journal of Sound and Vibration*, vol. 318, no. 4-5, pp. 655–662, dec 2008.

[43] S. Lenci, M. Brocchini, and C. Lorenzoni, "Experimental Rotations of a Pendulum on Water Waves," *Journal of Computational and Nonlinear Dynamics*, vol. 7, 2012.

[44] D. Yurchenko and P. Alevras, "Parametric pendulum based wave energy converter," *Mechanical Systems and Signal Processing*, vol. 99, pp. 504–515, 2018.

[45] V. Vaziri, A. Najdecka, and M. Wiercigroch, "Experimental control for initiating and maintaining rotation of parametric pendulum," *The European Physical Journal Special Topics 2014 223:4*, vol. 223, no. 4, pp. 795–812, apr 2014.

[46] F. Reguera, F. E. Dotti, and S. P. Machado, "Rotation control of a parametrically excited pendulum by adjusting its length," *Mechanics Research Communications*, vol. 72, pp. 74–80, mar 2016.

[47] S. Zou, O. Abdelkhalik, R. Robinett, U. Korde, G. Bacelli, D. Wilson, and R. Coe, "Model Predictive Control of parametric excited pitch-surge modes in wave energy converters," *International Journal of Marine Energy*, vol. 19, pp. 32–46, sep 2017.

[48] B. Orazov, O. M. O'Reilly, and S. Savaş, "On the dynamics of a novel ocean wave energy converter," *Journal of Sound and Vibration*, vol. 329, no. 24, pp. 5058–5069, nov 2010.

[49] G. Giorgi, "Computational performance of a fast nonlinear Froude-Krylov force calculation approach for axisymmetric and prismatic floaters," in *Proceedings of the European Wave and Tidal Energy Conference*, 2021, pp. 1898–1–1898–10.

[50] F. Carapellese, E. Pasta, B. Paduano, N. Faedo, and G. Mattiazzo, "Intuitive LTI energy-maximising control for multi-degree of freedom wave energy converters: The PeWEC case," *Ocean Engineering*, vol. 256, p. 111444, jul 2022.

[51] D. G. Gioia, E. Pasta, P. Brandimarte, and G. Mattiazzo, "Data-driven control of a Pendulum Wave Energy Converter: A Gaussian Process Regression approach," *Ocean Engineering*, vol. 253, p. 111191, jun 2022.

[52] G. Cervelli, L. Parrinello, C. Moscoloni, and G. Giorgi, "Comparison of the ERA5 Wave Forecasting Dataset Against Buoy Record," *Instrumentation Mesure Métrologie*, vol. 21, no. 3, pp. 87–95, 2022.

[53] A. Babarit and G. Delhommeau, "Theoretical and numerical aspects of the open source BEM solver NEMOH," *Proceedings of the 11th European Wave and Tidal Energy Conference.*, no. September 2015, pp. 1–12, 2015.

[54] I. WAMIT, "WAMIT User Manual," 2019.

[55] N. Faedo, Y. Peña-Sanchez, and J. V. Ringwood, "Finite-Order Hydrodynamic Model Determination for Wave Energy Applications Using Moment-Matching," *Ocean Engineering*, vol. 163, pp. 251–263, 2018.

[56] Y. Peña-Sanchez, N. Faedo, M. Penalba, G. Giorgi, A. Merigaud, C. Windt, D. Garc, L. Wang, and J. V. Ringwood, "Finite-Order hydrodynamic Approximation by Moment-Matching (FOAMM) toolbox for wave energy applications," *13th European Wave and Tidal Energy Conference*, 2019.

[57] G. Giorgi and J. V. Ringwood, "Relevance of pressure field accuracy for nonlinear Froude–Krylov force calculations for wave energy devices," *Journal of Ocean Engineering and Marine Energy*, vol. 4, no. 1, pp. 57–71, 2018.

[58] G. Giorgi, "Nonlinear Froude-Krylov Matlab demonstration toolbox," 2019.

[59] G. Giorgi and J. V. Ringwood, "Analytical formulation of nonlinear Froude-Krylov forces for surging-heaving-pitching point absorbers," in *ASME 2018 37th International Conference on Ocean, Offshore and Arctic Engineering*, Madrid, 2018.

[60] N. Faedo, G. Giorgi, J. V. Ringwood, and G. Mattiazzo, "Optimal control of wave energy systems considering nonlinear Froude–Krylov effects: control-oriented modelling and moment-based control," *Nonlinear Dynamics*, vol. 109, no. 3, pp. 1777–1804, 2022.